Mutations in the stereospecificity pocket and at the entrance of the active site of *Candida antarctica* lipase B enhancing enzyme enantioselectivity

Z. Marton [a], V. Léonard-Nevers [a], P.-O. Syrén [b], C. Bauer [a], S. Lamare [a], K. Hult [b], V. Tranc [c], M. Graber [a],*

[a] UMR CNRS 6250 LIENSs, Université de La Rochelle, Bâtiment Marie Curie, Avenue Michel Crépeau, 17042 La Rochelle cedex 1, France
[b] Department of Biochemistry, School of Biotechnology, Royal Institute of Technology, AlbaNova University Center, SE-106 91 Stockholm, Sweden
[c] UMR CNRS 6204 U3B, Faculté des Sciences et Techniques, 2 rue de la Houssinière, 44322 Nantes cedex 3, France

ARTICLE INFO

ABSTRACT

Two different parts of *Candida antarctica* lipase B (stereospecificity pocket at the bottom of the active site and hydrophobic tunnel leading to the active site) were redesigned by single- or double-point mutations, in order to better control and improve enzyme enantioselectivity toward secondary alcohols. Single-point isosteric mutations of Ser47 and Thr42 situated in the stereospecificity pocket gave rise to variants with doubled enantioselectivity toward pentan-2-ol, in solid/gas reactor. Besides, the width and shape of the hydrophobic tunnel leading to the active site was modified by producing the following single-point mutants: Ile189Ala, Leu278Val and Ala282Leu. For each of these variants a significant modification of enantioselectivity was observed compared to wild-type enzyme, indicating that discrimination of the enantiomers by the enzyme could also arise from their different accessibilities from the enzyme surface to the catalytic site.
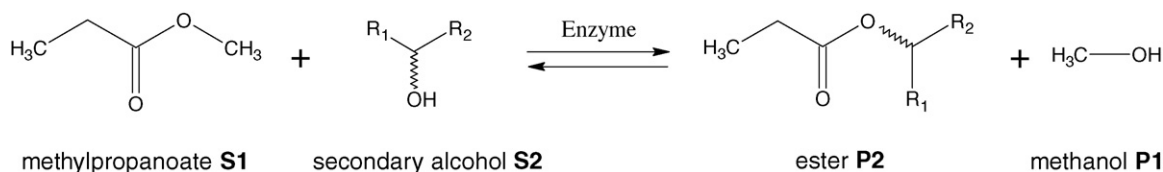
1. Introduction

It is now well-known that enantioselectivity of lipases can be modified by structural factors of the substrates and of the enzyme. In this context, directed mutagenesis has been used a lot to improve lipases enantioselectivity and to increase the understanding of how these enzymes solve the task of distinguishing between enantiomers [1–4]. Especially, lipase B from *Candida antarctica* (CALB) has been studied a lot by this way [5,6]. In this present work our goal has been to better understand structural determinants of CALB enantioselectivity toward secondary alcohols and to obtain more-selective mutants. Crystal structure analysis of CALB reveals a rather narrow and deep active site with a small stereospecificity pocket flanked by residues Thr42, Ser47 and Trp104, which is at the origin of its enantioselectivity [7,8]. The strong *R*-selectivity of CALB toward secondary alcohols is explained by the different binding modes of the enantiomers in the stereospecificity pocket [9,10]. The fast-reacting enantiomer positions its medium-sized substituent in the stereospecificity pocket and its large substituent toward the active site entrance. The slow-reacting enantiomer has to get into position in the active site in the opposite way, in order to form a catalytically active binding mode, although the largest substituent is not easily fitted in the stereospecificity pocket. This steric limitation makes CALB very selective toward secondary alcohols with

a medium substituent not larger than an ethyl group and a large substituent bigger than an ethyl group.

Nevertheless, Rotticci et al. showed that steric interaction in the stereospecificity pocket is not the only important factor for the discrimination between enantiomers. These authors produced CALB variants with nearly isosteric mutations in the stereospecificity pocket (Thr42Val, Ser47Ala and Thr42Val/Ser47Ala) and obtained an increased enantioselectivity towards 1-bromo-2-octanol and 1-chloro-2-octanol, when the single- or double-point mutation Ser47Ala was used [6]. This effect was ascribed to a decrease of electrostatic repulsion between the halogen atom of the substrate and the stereospecificity pocket induced by the mutation. In the present paper, the effect of the same isosteric mutations in the stereospecificity pocket was further studied in a solid–gas bioreactor, for the CALB-catalyzed resolution of linear secondary alcohols (Scheme 1). Moreover, for these variants, variations in activation enthalpy and entropy were measured, and the effect of water on selectivity was studied, in the same type of reactor. This reactor includes the enzyme at a solid state forming a fixed bed, and gaseous substrates and nitrogen as carrier gas percolating the enzymatic bed. The reactor presents the advantage to independently control the thermodynamic activities of the components present in the reaction medium by varying the partial pressure of each compound in the carrier gas that percolates through the catalytic bed [11]. Moreover this type of reactor permits the determination of the specific water addition in the medium, by adding water in the gaseous stream at a controlled thermodynamic activity [12,13].

* Corresponding author. Tel.: +33 5 46 45 86 30; fax: +33 5 46 45 82 65.
E-mail address: mgraber@univ-lr.fr (M. Graber).

Scheme 1.

Finally, we focused on the narrow and short tunnel leading to CALB active site, and bounded by four hydrophobic residues, Ile189, Leu278, Ala282 and Ile285. As substrates have to cross this tunnel before the formation of the second tetrahedral intermediate, we tested the ability of these hydrophobic amino acids to play a role in the discrimination between enantiomers. By using different single-point mutations, the access of linear secondary alcohols to the active site was made more difficult by increasing the volume of Ala282 at the active site entrance (variant Ala282Leu), or easier by decreasing the volume of Leu278 or Ile189 (variants Leu278Val and Ile189Ala). The only study mentioning the discrimination of the enantiomers through their channeling from the enzyme surface to the catalytic triad, concerns *Burkholderia cepacia* lipase in the case of the resolution of (*R*, *S*)-2-bromophenyl acetic acid ethyl ester by transesterification in the presence of octanol [14]. Such an investigation has never been performed in case of CALB lipase and is presented in this paper, by studying the enantioselectivity of CALB variants with single-point mutations at the entrance of the active site crevice.

2. Experimental

2.1. Chemicals

Substrates and other chemicals were purchased from Sigma–Aldrich-Fluka Chemical Co. They were of the highest purity available (98% minimum) and checked by gas chromatography before use. Substrates were dried by distillation under argon prior to use and stored under argon atmosphere and over molecular sieves. Solvents were purchased from Carlo Erba. 1-Methylpropylpropanoate, 1-methylbutylpropanoate, 1-methylpentylpropanoate, 1-ethylpentylpropanoate and 1-ethylhexylpropanoate were synthesized from corresponding alcohol and propanoic acid in presence of *p*-toluene sulfonic acid and molecular sieves [15]. 1-Methylhexylpropanoate and 1-methylheptylpropanoate were obtained from the corresponding alcohol and propanoic anhydride in pyridine at room temperature [16]. High purity water was obtained with the MilliQ system (Millipore, France).

2.2. Enzyme

2.2.1. Wild-type (WT) and stereospecific pocket mutants

WT CALB and stereospecificity pocket variants (Ser47Ala, Thr42Val and Ser47Ala–Thr42Val) were produced in the methylotropic yeast *Pichia pastoris*. These lipases were expressed extracellularly and purified from the medium by hydrophobic interaction chromatography, followed by gel filtration [6,17].

Enzyme adsorption was performed onto 60–80 mesh Chromosorb P AW DMCS (acid washed dimethylchlorosilanized) (Varian, France). In a typical adsorption procedure for solid/gas catalysis, WT enzyme (0.106 mg) or variant (0.85 mg) was dissolved in sodium phosphate buffer (pH 7.5, 10 mM), and dry Chromosorb P AW DMCS (1 g) was added to the solution. The amount of immobilized enzyme was determined by measuring absorbance at 280 nm, by taking a molar extinction coefficient equal to $40690\,M^{-1}\,cm^{-1}$. After vigorous shaking, the preparation was left for 1 week under vacuum and over P_2O_5 at room temperature.

2.2.2. Mutants of the entrance crevice

The three mutants Ile189Ala, Leu278Val and Ala282Leu were obtained through site-directed mutagenesis [18]. The pGAPZα B plasmid was amplified by polymerase chain reaction (PCR) with the mutagenic primers designed to be non-overlapping at the ends [19]. The product of PCR was analysed on 1% agarose gel and was used to transform *E.coli* XL-1 blue cells. Colonies containing the wished mutation were identified by sequencing and used to produce the plasmid in large quantity (i.e. >20 μg) using QIAPrep Spin miniprep (QIAGEN GmbH, Hilden, Germany). Plasmids were linearized and used to transform *P. pastoris* SMD 1168 H by electroporation. Transformants of *P. pastoris* were cultured in order to produce CALB mutants. The enzyme contained in the supernatant was purified on butyl sepharose FF column. Purified protein fractions were subjected to buffer exchange to 50 mM potassium phosphate buffer, pH 7.5 and freeze dried.

0.53 mg enzyme was dissolved in 1 mL of MilliQ water, and dry Chromosorb P AW DMCS (1 g) was added to the solution. After vigorous shaking, the preparation was left for 1 week under vacuum and over P_2O_5 at room temperature.

2.3. Experimental setup for solid–gas catalysis

The bioreactor used in this study has already been described in a previous publication [20]. Thermodynamic experiments were run from 308 to 363 K with immobilized enzyme preparation (10–200 mg). All other experiments were made at 318 K. The total flow rate passing through the reactor was set to 800 μmol/min for thermodynamic study, 1000 μmol/min for entrance crevice mutations effects study and 1150 μmol/min for water effects study. Methyl propanoate and secondary alcohols thermodynamic activities in the solid/gas reactor were fixed at 0.1 and 0.05, respectively, except for experiments with heptan-3-ol and octan-3-ol, for which thermodynamic activities for alcohol was fixed at 0.1 and 0.2 for methyl propanoate.

2.4. Chromatographic assays

For the solid/gas system analyses, the vapour phase leaving the bioreactor was sampled by using a loop (0.25 mL) on a six-way valve (Valco) maintained at 175 or 220 °C. Samples were automatically injected into the split injector of a gas chromatograph (Agilent 6890N) (split 2:1) equipped with a flame ionization detector (FID) for the detection of all products. The column was a Chirasil-DEX CB (25 m, 0.25 mm i.d., 0.25 μm β-cyclodextrin; Chrompack, France). Separation methods depended on the substrate used. Column temperature was 55 °C for 20 min (1.5 mL/min, 180 °C, 180 °C) with butan-2-ol, 55 °C for 15 min, 3 °C/min, 85 °C (1.5 mL/min, 180 °C, 180 °C) with pentan-2-ol, or 50 °C for 30 min (1.8 mL/min, 250 °C, 250 °C) when water was added, 60 °C for 15 min, 3 °C/min, 90 °C for 5 min (2 mL/min, 180 °C, 180 °C) with hexan-2-ol and hexan-3-ol, 60 °C for 15 min, 3 °C/min, 90 °C for 5 min (2 mL/min, 200 °C, 200 °C) with heptan-2-ol and heptan-3-ol, 70 °C for 15 min, 3 °C/min, 100 °C for 5 min (2 mL/min, 200 °C, 200 °C) with octan-2ol, and 90 °C

Table 1

Thermodynamic components of the enantiomeric ratio, E, and activity A (μmol of product min^{-1} mg^{-1} of free enzyme) for acylation of pentan-2-ol with methyl propanoate as acyl donor, catalyzed by WT *Candida antarctica* lipase B and the three variants of the stereospecificity pocket. All experiments were performed at a_w equal to 0 in the gaseous stream of the solid/gas reactor. For measurements of both E- and A- values the thermodynamic activity of methyl propanoate and alcohol were fixed at 0.1 and 0.05, respectively.

Type of enzyme	A	E at 318 K[a]	$\Delta_{R-S}\Delta G^*$ at 318 K [kJ mol^{-1}][b]	$\Delta_{R-S}\Delta H^*$ [kJ mol^{-1}][c]	$-T\Delta_{R-S}\Delta S^*$ [kJ mol^{-1}][d]	$\Delta_{R-S}\Delta S^*$ [J K^{-1} mol^{-1}][c]	N[e]
WT[f]	30	101 ± 5	−12.2 ± 0.1	−18 ± 1.2	6 ± 1.3	−19 ± 4	18
Thr42Val	7.5	236 ± 6	−14.4 ± 0.2	−11 ± 0.7	−3 ± 0.5	11 ± 2	16
Ser47Ala	10	198 ± 19	−14 ± 0.6	−20 ± 1.0	6 ± 0.9	−19 ± 3	11
Thr42Val–Ser47Ala	2.3	98 ± 13	−12.1 ± 0.4	−11 ± 0.7	−1 ± 0.6	3 ± 2	13

[a] Standard deviations were calculated with three values of E, and correspond to 95% confidence intervals.

[b] Values calculated from −RT Ln E. Standard deviations were obtained from the standard deviations of E.

[c] $\Delta_{R-S}\Delta H^*$ and $\Delta_{R-S}\Delta S^*$ were calculated by using the least square method, with between 11 and 18 measurement of E as a function of T. Standard deviations correspond to 99% confidence intervals.

[d] $-T\Delta_{R-S}\Delta S^*$ values were calculated at 318 K. Standard deviations were obtained from standard deviations of $\Delta_{R-S}\Delta S^*$.

[e] Total number of E measurements.

[f] Results of this line have already been published in a previous publication [12].

for 17 min (2 mL/min, 200 °C, 200 °C) for octan-3-ol. Nitrogen was used as the carrier gas with a constant flow rate (between 1.5 and 2 mL/min according to experiments). Hydrogen and air were supplied to the FID at 35 and 350 mL/min respectively. Quantitative data were obtained by integration on an Agilent 3396 Series III integrator or on GC Chemstation Rev B.03.02. The external calibrations of the substrates were carried out by programming a range of their partial pressures in the bioreactor, and by gas chromatography analysis. For the products (methanol and chiral esters), an internal calibration was carried out by using methyl propanoate and corresponding alcohol as internal standards. For accurate determination of E-values the vapour phase leaving the bioreactor was condensed. Elution peaks of (R)-pentan-2-ol and (S)-pentan-2-ol were identified by using commercial pure (R)-pentan-2-ol. Retention time of the reaction products was obtained by adding chemically synthesized esters (R, S), as described in Section 2.1. The absolute configuration of the reaction products was established by esterification of commercial pure alcohol enantiomers.

2.5. Determination of the enantiomeric ratio

The enantiomeric ratio, E, was calculated from ee$_s$ and ee$_p$ [21,22]. The E-values were based on the average of three measurements for each condition; in all cases the standard deviation was less than 10%. The equations RT ln $E = -\Delta_{R-S}\Delta G^*$ and $\Delta_{R-S}\Delta G^* = \Delta_{R-S}\Delta H^* - T\Delta_{R-S}\Delta S^*$ were used to calculate enthalpic and entropic components of E [23,24].

2.6. Shape of active site and entrance tunnel

The crystal structure of native CALB was obtained from the Protein Data Bank [25] (PDB entry: 1TCA; resolution 1.55 Å [26]). All molecular modeling visualizations, mutations and calculations were performed with CHARMM force field [27] using the program-package Discovery Studio (DS) version 1.6 or 2.1 (Accelrys Inc.). Systematic rotamer search was performed on crystal structure using Richardson rotamer library [28]. Conolly surface [29] of the sum of all possible rotamers for a residue was calculated at a probe radius of 1.4 Å.

Structure of second tetrahedral intermediate formed (R)-heptan-3-ol:complex enzyme-(R)-1-ethylpentylpropanoate shown in Fig. 4, was obtained from a structure previously obtained with (S)-hexan-3-ol:complex enzyme-(S)-1-ethylbutylpropanoate, by manual modifications followed by Steepest Descent minimizations (RMSD ≤ 0.01). This last structure was obtained from crystal structure of CALB by manual construction, after removal of crystallographic water molecules, followed by MD simulation carried out by adopting a 12 Å non-bound spherical cut-off, using the isothermal–isochoric ensemble (NVT) [30]

and without solvents. The Standard Dynamics Cascade Protocol of DS 1.6 was used with a time step of 1 fs. The complex was energy minimized (2500 Steepest descent and 2500 adobted Basis NR) and temperature of the system was raised from 50 to 400 K over 2 ps. After a short equilibration (1 ps) a production run was carried out for 10 ps at 400 K. Backbone atoms were kept fixed during simulation, in order to keep the original structural integrity.

3. Results and discussion

3.1. The effect of two point mutations in the stereospecificity pocket of CALB

Acyl-transfer reaction rates, in case of catalysis by native or modified CALB, were experimentally measured with methyl propanoate as acyl donor and pentan-2-ol as racemic nucleophile, in a continuous solid gas reactor at 318 K, at water activity close to zero. The acyl-transfer activity decreased by factors 3 and 4, when using respectively Ser47Ala and Thr42Val mutants, compared to WT CALB, for which a value of 30 μmol of product min^{-1} and mg^{-1} of pure and free enzyme was found. It decreased by a factor 13 when using double mutant Ser47Ala–Thr42Val. These results can be compared with the ones obtained by Rotticci et al. with tributyrin as substrate in aqueous media. In this case activity decreased by factors 1.8, 6 and 3 compared to WT CALB when using respectively Ser47Ala, Thr42Val and Ser47Ala–Thr42Val mutants [6].

The enantioselectivity of these different enzymes toward pentan-2-ol was also measured in the solid gas reactor. The E-value significantly increased when using Ser47Ala and Thr42Val mutants, reaching respectively 198 and 236, instead of 100 with WT enzyme [12]. On the other hand, double mutant Ser47Ala–Thr42Val presented an enantioselectivity toward pentan-2-ol very close to that of the WT enzyme. Furthermore, a thermodynamic analysis of enantioselectivity was performed by considering both activation enthalpy and entropy (Table 1). It can be seen that the preferred enantiomer (R)-pentan-2-ol, was favored by enthalpy ($\Delta_{R-S}\Delta H^* < 0$) but disfavored by entropy ($\Delta_{R-S}\Delta S^* < 0$) in case of WT enzyme and Ser47Ala variant. In case of Thr42Val and Ser47Ala–Thr42Val variants, enantioselectivity is favored both by enthalpy and entropy.

These different results show that single- or double-point mutations in the stereospecificity pocket have very significant effects both on activity and selectivity of CALB. Moreover, thermodynamic analysis reveals that these effects are complex, as mutations lead to modifications of both activation enthalpy and entropy differences between R- and S-enantiomers. The importance of the entropy contribution in defining enantioselectivity is once again shown [31], but the exact molecular mechanism of how entropy and flexibility are related to enzyme activity and selectivity is still elusive.
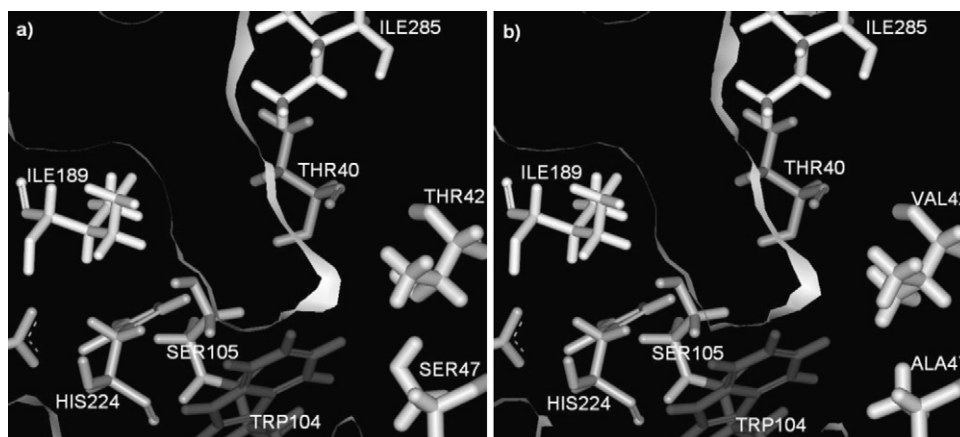
Fig. 1. Stereospecificity pocket of CALB: (a) WT; and (b) double mutant Thr42ValSer47Ala.

In the present study, the effects of mutations cannot be ascribed to modifications of the size of the stereospecificity pocket, as threonine and valine on the one side are isosteric, and serine and alanine on the other side, have similar molar volumes. Therefore the mutations did not lead to major changes in the size of the stereospecificity pocket (Fig. 1). Counterexample can be found in the literature in which mutation effects is directly related to a change of the stereospecificity pocket size: the Trp104Ala mutation of CALB increases very significantly the size of the stereospecificity pocket, and this redesigned pocket was found to accommodate much larger groups than the WT enzyme. This change transformed the strongly R-selective WT CALB into an S-selective mutant for the resolution of 1-phenylethanol [32].

Besides, the change in hydrophobicity of the stereospecificity pocket of CALB caused by the Thr42Val and the Ser47Ala mutations cannot either be considered as a reason for variation of enantioselectivity toward pentan-2-ol, as it was shown that substrate selectivity of these mutants was very similar to that of the WT enzyme, for the acylation of symmetrical secondary alcohols (propan-2-ol, pentan-3-ol and heptan-4-ol) [18]. On the contrary, in case of resolution of halohydrins through CALB-catalyzed acylation, the change of hydrophobicity promoted by Thr42Val and Ser47Ala mutations affected the CALB selectivity toward the halodrins, by decreasing electrostatic repulsion between substrates and enzyme [6].

The increase of enantioselectivity toward pentan-2-ol afforded by single-point mutations (Thr42Val and Ser47Ala) may originate from modification of the H-bond network between amino acid residues in the vicinity of the stereospecificity pocket, and different spatial degrees of freedom and mobility of these residues and also of substrate substituent positioned in this pocket. The higher E-value for the single-point mutants compared to that of the WT could arise from higher mobility of the non-mutated residue, which now is not hydrogen bonded and has more mobility. If it moves more than in the WT, the specificity pocket will be smaller, then the S-enantiomer will not fit so well and E goes up. The H-bond network progress and mobility of the residues located in the stereospecificity pocket, when using variants Thr42Val and Ser47Ala, compared to WT CALB, will be the topic of future studies by molecular dynamics simulation.

3.2. The effect of water on enantioselectivity of the stereospecificity pocket variants

The effect of water thermodynamic activity (a_w) on WT CALB-catalyzed acyl-transfer reaction was previously extensively studied by using a solid/gas reactor [12,13]. It was shown that water had a pronounced effect on CALB activity and enantioselectivity. E-value increased from 100 at water activity close to zero, in case of the resolution of pentan-2-ol at 318 K, to a maximum of 320, at water activity of 0.2. In this part, we were intending to compare the effect of water on the enantioselectivity toward pentan-2-ol at 318 K, of Thr42Val, Ser47Ala and Thr42Val–Ser47Ala variants with the results previously obtained for the WT enzyme. Results are shown in Fig. 2. First, enantioselectivity increases in all cases up to $a_w = 0.1$ for Ser47Ala, $a_w = 0.08$ for Thr42Val, and $a_w = 0.3$ for Thr42Val–Ser47Ala to reach the respective following maxima: $E = 449$, 567 and 289. Above a_w values corresponding to maximal E, enantioselectivity decreases, after a plateau for Ser47Ala variant in the range of a_w from 0.1 to 0.3.

So it appears that the enhancement of E promoted by water is significantly reduced in case of double-point variant compared to WT enzyme, whereas it is strongly enhanced in case of single-point variants.

Previously, the increase of enantioselectivity of WT CALB for pentan-2-ol at low water activity, has been interpreted by specifically binding of a water molecule in the stereospecificity pocket, leading to a reduction of its size and thereby rendering binding of S-enantiomer still more difficult compared to the R-form [12].
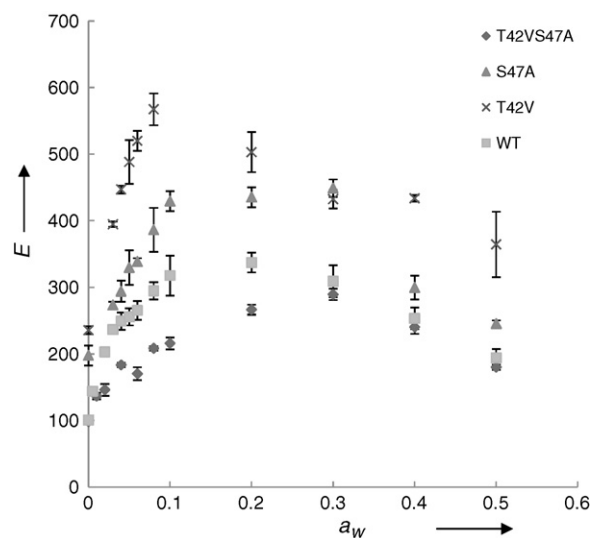

Fig. 2. Influence of thermodynamic water activity, a_w on enantioselectivity at 318 K for the acylation of pentan-2-ol with methyl propanoate as acyl donor, catalyzed by WT CALB and three variants Thr42Val, Ser47Ala and Thr42ValSer47Ala, in continuous solid/gas reactor.
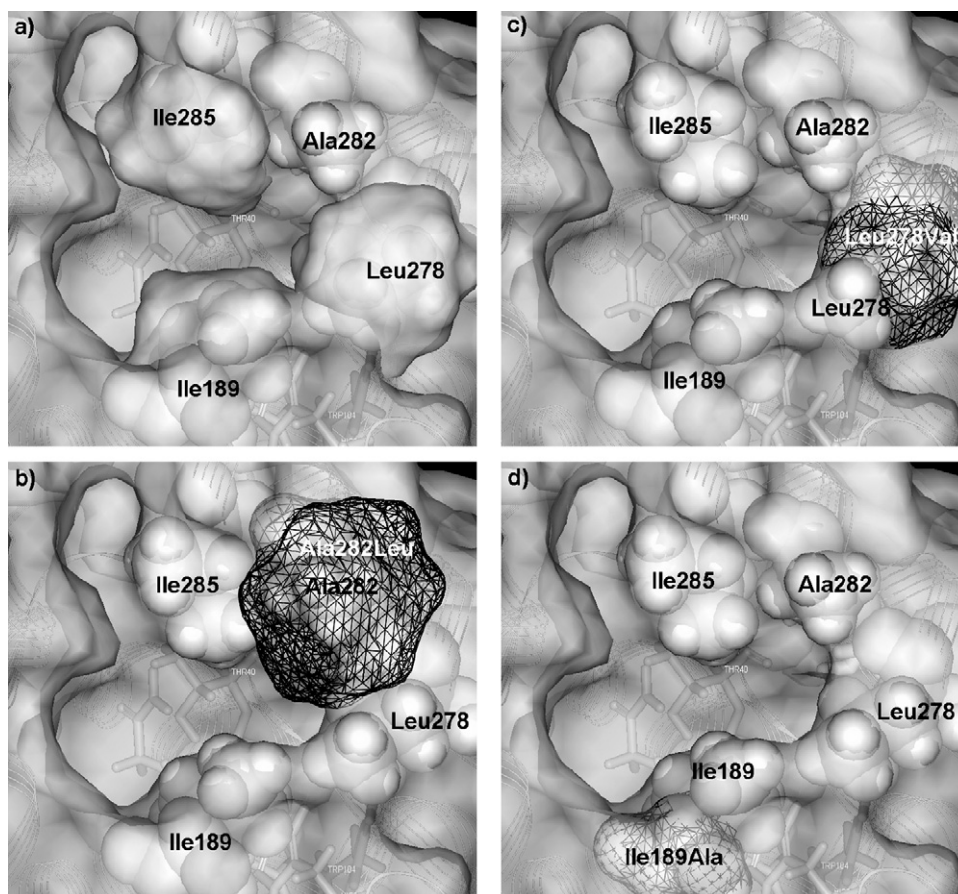
Fig. 3. Shape of the entrance tunnel. (a) WT with occupancy of hydrophobic residues: Ile189, Leu278, Ala282 and Ile285 (surface of all rotamers); (b) mutant Ala282Leu; (c) mutant Leu278Val; and (d) mutant Ile189Ala; occupancy of mutants in black grid.

The result obtained with double-point variant Thr42Val–Ser47Ala showing a significant decrease of water effect, is in accordance with this hypothesis, as the redesigned stereospecificity pocket is not water-attractive anymore, because both mutations lead to the replacement of a polar hydroxyl group by an apolar substituent (methyl or hydrogen atom). This fact can be confirmed by calculating the water dissociation constant with specificity pocket (K_d), thanks to a Hill equation analysis for $a_w < 0.1$. K_d for Thr42Val–Ser47Ala variant was found to be equal to 0.1, which is much higher than the value of 0.03 previously obtained with WT enzyme. The Hill coefficient for double mutant ($h = 0.55$) was consistent with one water molecule bound in the stereospecificity pocket as for the WT enzyme [12]. Finally, the fact that maximal E-value was obtained at higher water activity for Thr42Val–Ser47Ala variant compared to WT is also consistent with a lower affinity for water.
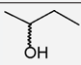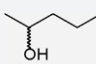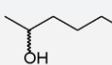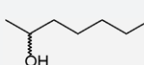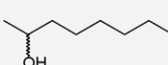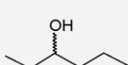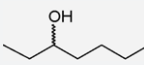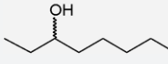
On the contrary, in case of single-point variants, the Hill equation analysis gave much lower K_d values than that obtained for the WT enzyme: $K_d = 0.004$ and 0.0002 for Ser47Ala and Thr42Val respectively, with Hill coefficients being respectively equal to 1.45 and 2.24. These results are in agreement with a high affinity for water for the stereospecificity pocket of single-point variants, leading to a strong enhancement of E-value when going from water activity close to zero to 0.1 for Ser47Ala or 0.08 for Thr42Val.

These very high E-values are promoted by water at very low activity, where water acts mainly through specifically located effects. At higher water activity, entropic effects coming from water molecules have been shown to become predominant and can lead to a decrease of E [13].

3.3. The effect of mutations at the entrance of the active site of CALB

The crystallographic structure of CALB shows that the substrate binding pocket is an elliptical, steep funnel. The pocket constitution is similar to other lipases with a hydrophilic bottom of the funnel, which is formed by the catalytic Ser105 and residues of the oxyanion hole, Thr40 and Gln106 [33]. Near the surface the pocket is bordered by hydrophobic residues, which interact with organic solvents, but unlike to lipases, CALB have no lid and is not submitted to interfacial activation. The active site crevice can be partitioned into two sides, an acyl side and an alcohol side, where the corresponding parts of the substrate will be located during catalysis [7]. The alcohol side is bounded by four hydrophobic residues, Ile189, Leu278, Ala282 and Ile285. They form a narrow tunnel, which must be crossed by substrate before the formation of the second tetrahedral intermediate. The volumes occupied by these residues were calculated by systematic conformational search. This study showed that these residues have side chains free to rotate and have no steric interaction with neighboring residues (Fig. 3a). Consequently a concerted motion of the side chains cannot be observed, whereas such was the case with *B. cepacia* lipase, when the substrate passes though the bottleneck formed by Val266 and Leu17 [14]. However Fig. 3a suggests that these four hydrophobic residues, Ile189, Leu278, Ala282 and Ile285 can affect substrate trajectory. Mutations were considered in order to understand the role of these residues in the selectivity of CALB. To avoid electrostatic effects, only mutations in another aliphatic hydrophobic residue were considered. The volume of residue 282 was expended by changing native Ala into Leu, and volumes of

Table 2

Enantiomeric ratio E[a] and activity A (μmol of product min^{-1} and mg^{-1} of free enzyme) for acylation of chiral secondary alcohols with methyl propanoate as acyl donor at 318 K, in solid/gas reactor, catalyzed by WT *Candida antarctica* lipase B and variants of CALB obtained by mutations of amino acids at the entrance of the active site crevice. All experiments were performed at a_w equal to 0 in the gaseous stream of the solid/gas reactor. Thermodynamic activity of methyl propanoate and alcohol were fixed at 0.1 and 0.05, respectively, except for heptan-3-ol and octan-3-ol (0.2 and 0.1), for measurements of both E- and A-values.

Structure	WT		Ala282Leu		Leu278Val		Ile189Ala	
	E	A	E	A	E	A	E	A
butan-2-ol	4.6 ± 0.1	n.d.	4.9 ± 0.1	20.7	$5.8 \pm .0.2$	20.5	6.9 ± 0.4	12.3
pentan-2-ol	100 ± 6	17.7	130 ± 1	22.6	98 ± 8	29.1	87 ± 1	12.6
hexan-2-ol	297 ± 9	13.5	228 ± 8	26.1	216 ± 7	18.2	211 ± 6	10.8
heptan-2-ol	476 ± 30	11.7	337 ± 2	20.9	299 ± 18	11.1	437 ± 25	4.8
octan-2-ol	435 ± 18	6.7	298 ± 11	11.1	227 ± 3	7.2	400 ± 10	4.3
hexan-3-ol	78 ± 5	8.7	103 ± 8	9.8	83 ± 3	6.4	45 ± 3	2.8
heptan-3-ol	318 ± 15	2.4	208 ± 14	2.2	203 ± 15	1.8	192 ± 7	1.7
octan-3-ol	523 ± 31	3.1	245 ± 15	4.1	210 ± 15	3.3	199 ± 14	2.0

[a] Standard deviations were calculated with 5–12 values of E from two condensates, and correspond to 95% confidence intervals.

positions 278 and 189 were decreased by respectively changing Leu into Val and Ile into Ala (Fig. 3b–d). Ile189Ala, Leu278Val and Ala282Leu mutants were produced and their activity and enantioselectivity toward different chiral alcohols tested in solid/gas bioreactor.

Acyl-transfer reaction rates were experimentally measured with methyl propanoate as acyl donor and eight different linear secondary alcohols ranging from four to eight carbons as racemic nucleophile, at 318 K and water activity close to zero. Results showed that activity increased by a factor 1.1–2, when using Ala282Leu variant compared to WT CALB, except for heptan-3-ol, for which it decreased; activity was similar or slightly increased when using Leu278Val variant, except for hexan-3-ol and heptan-3-ol, for which it decreased, and activity decreased with Ile189Ala mutant. As an example, in case of hexan-2-ol as nucleophile, a value of 13.5 μmol of product min^{-1} mg^{-1} of pure and free enzyme was found with WT CALB, which was doubled to 26.1 with Ala282Leu, increased to 18.2 with Leu278Val and decreased to 10.8 with Ile189Ala.

Table 2 shows the results for the enantiomeric ratio E for acylation of the eight chiral alcohols (butan-2-ol, pentan-2-ol, hexan-2-ol, heptan-2-ol, octan-2-ol, hexan-3-ol, heptan-3-ol and octan-3-ol), catalyzed by WT CALB or the different variants of CALB with mutations at the entrance of the active site crevice. It appears that all mutations have a significant effect on E, promoting an increase of E up to a factor 1.5 or a decrease up to a factor 2.2. Nevertheless the upward or downward trend for E is variable for each mutation, depending on the length of the large substituent of the chiral alcohol. So another time, the analysis of the results for E variations is complex and needs to consider many different structural causes.

To analyze these data, the following postulate can be formulated: modifications of the entrance crevice to the active site by mutations of amino acids, will predominantly affect the trajectory of the *S*-enantiomer, as this substrate has to enter the active site with its large substituent in the front, in order to react. Indeed, according to the model proposed by Haeffner et al., the *S*-enantiomer has to put its large substituent into the stereospecificity pocket, located at the bottom of the active site, in order to form catalytically active second tetrahedral intermediate [9]. This last covalent intermediate is considered to be a good model of the transition state intermediate in case of CALB-catalyzed resolution of chiral nucleophile by acyl-transfer [9].

As shown in the following discussion, this postulate provides a rational explanation for most results. In some cases however, other structural explanations have to be given, like a modification of the *R*-enantiomer trajectory also, an effect of the mutation on the structure and energy state of second tetrahedral intermediate or an interaction between acyl part and residue 189, which are very close together. In any case, a complete structural explanation of the effect of mutations on E very likely involves a combination of these different individual effects. Molecular dynamics simulations are currently in progress to study substrate trajectory in WT and variants of CALB.

According to the above postulate, Leu278Val mutant is supposed to make access of *S*-enantiomer to the active site easier, because of the smaller size of Val compared to Leu. This hypothesis is verified (lower E-value than WT enzyme) for hexan-2-ol, heptan-2-ol, octan-2-ol, heptan-3-ol and octan-3-ol. So, if the large substituent of linear secondary alcohol includes four or more C, then the postulate is verified. If the large substituent includes three C or less, the observed effect is not in agreement with the postulate: higher E-value than WT enzyme (butan-2-ol and hexan-3-ol) or similar E-value (pentan-2-ol). In these cases, an easier access to the active site for the *R*-enantiomer could explain the effect.

Ile189Ala mutant is also supposed to ease access of *S*-enantiomer to the active site. This hypothesis is verified (lower E-value than WT enzyme) for all alcohols except butan-2-ol. So if
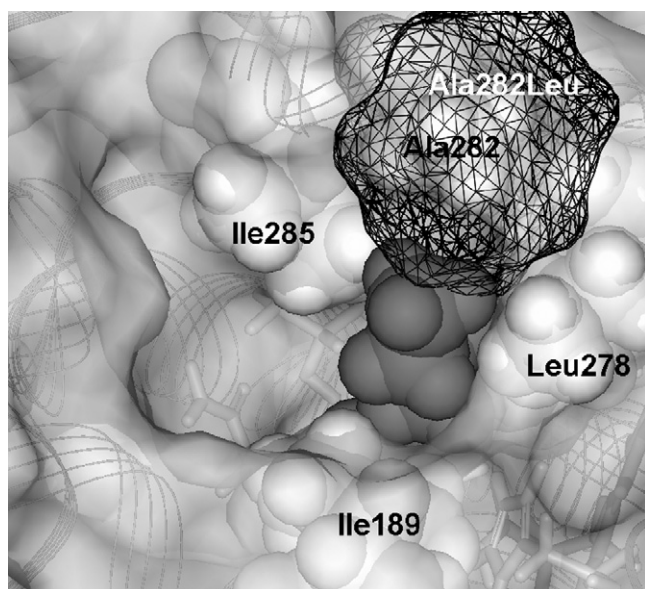
Fig. 4. Structure of WT and Ala282Leu CALB with (R)-1-ethylpentylpropanoate covalently attached to Ser105 (second tetrahedral intermediate formed with (R)-heptan-3-ol), obtained by MD simulation described in Section 2.6; occupancy of mutants in black grid, (R)-1-ethylpentylpropanoate in dark grey.

the large substituent of linear secondary alcohol includes three or more C, then the postulate is verified.

For the Ala282Leu variant, our postulate implies a more difficult access of the S-enantiomer to the active site, because of the steric hindrance of the crevice caused by Leu282 replacing Ala. The postulate is verified (higher E-value than WT enzyme) for butan-2-ol, pentan-2-ol and hexan-3-ol. So, if the large substituent of linear secondary alcohol includes three C or less, then the postulate is verified. If the large substituent includes more than three C (hexan-2-ol, heptan-2-ol, octan-2-ol, heptan-3-ol, octan-3-ol), the observed effect is opposite to the one predicted by the postulate: lower E-value than WT enzyme. In these cases, a more difficult access to the active site for the R-enantiomer could explain the effect or also an interaction between the large substituent of the R-enantiomer and the residue Leu282, during formation of the second tetrahedral intermediate. Fig. 4 shows an example of such an interaction in case of the second tetrahedral intermediate formed with (R)-heptan-3-ol:(R)-1-ethylpentylpropanoate covalently attached to Ser105, with WT or Ala282Leu CALB.

4. Conclusion

In this paper, thanks to single-point mutations, new amino acid positions important for CALB enantioselectivity were identified at the entrance of the active site and offered altered enantioselectivity. Moreover, the crucial role of residues situated in the stereospecificity pocket was confirmed and resolution of pentan-2-ol could be improved, by using variants of this pocket. The present investigation is a new demonstration of the possibilities offered by protein redesign, for improving kinetic resolution using CALB. It also highlights that entropic phenomena, including enzyme and substrate flexibility, are crucial for understanding molecular mechanism of enzyme activity and selectivity, and remain to be accurately elucidated.

References

[1] M. Holmquist, M. Martinelle, P. Berglund, I.G. Clausen, S. Patkar, A. Svendsen, K. Hult, J. Protein Chem. 12 (1993) 749.
[2] H. Scheib, J. Pleiss, P. Stadler, A. Kovac, A.P. Potthoff, L. Haalk, F. Spener, F. Paltauf, R.D. Schmid, Protein Eng. 11 (1998) 675–682.
[3] F. Secundo, G. Carrea, C. Tarabiono, P. Gatti-Lafranconi, S. Brocca, M. Lotti, K.-E. Jaeger, M. Puls, T. Eggert, J. Mol. Catal. B: Enzym. 39 (2006) 166–170.
[4] F. Bordes, E. Cambon, V. Dossat-Létisse, I. André, C. Croux, J.-M. Nicaud, A. Marty, ChemBioChem 10 (2009) 1705–1713.
[5] A. Magnusson, K. Hult, M. Holmquist, J. Am. Chem. Soc. 123 (2001) 4354–4355.
[6] D. Rotticci, J.C. Rotticci-Mulder, S. Denman, T. Norin, K. Hult, ChemBioChem 2 (2001) 766–770.
[7] J. Uppenberg, N. Ohrner, M. Norin, K. Hult, G.J. Kleywegt, S. Patkart, V. Waagen, T. Anthonsen, T.A. Jones, Biochemistry 34 (1995) 16838–16851.
[8] C. Orrenius, F. Haeffner, D. Rotticci, N. Ohrner, T. Norin, K. Hult, Biocatal. Biotransfor. 16 (1998) 1–15.
[9] F. Haeffner, T. Norin, K. Hult, Biophys. J. 74 (1998) 1251–1262.
[10] D. Rotticci, F. Haeffner, C. Orrenius, T. Norin, K. Hult, J. Mol. Catal. B: Enzym. 5 (1998) 267–272.
[11] S. Lamare, M.-D. Legoy, M. Graber, Green Chem. 6 (2004) 445–458.
[12] V. Léonard, L. Fransson, S. Lamare, K. Hult, M. Graber, ChemBioChem 8 (2007) 1–7.
[13] V. Léonard-Nevers, Z. Marton, S. Lamare, K. Hult, M. Graber, J. Mol. Catal. B: Enzym. 59 (2009) 90–95.
[14] D. Guieysse, C. Salagnad, P. Monsan, M. Remaud-Simeon, V. Tran, Tetrahedron Asymm. 14 (2003) 1807–1817.
[15] C.E. Rehberg, Org. Syn. Coll. 3 (1955) 146.
[16] M.B. Smith, J. March, Advanced Organic Chemistry: Reactions, Mechanisms and Structure, 5th ed., Wiley, New York, 2001.
[17] J.C. Rotticci-Mulder, M. Gustavsson, M. Holmquist, K. Hult, M. Martinelle, Protein Expression Purif. 21 (2001) 386–392.
[18] A.O. Magnusson, J.C. Rotticci-Mulder, A. Santagostino, K. Hult, Chembiochem 6 (2005) 1051–1056.
[19] L. Zheng, U. Baumann, J.L. Reymond, Nucleic Acids Res. 32 (2004) e115.
[20] S. Lamare, M.D. Legoy, Biotechnol. Bioeng. 45 (1995) 387–397.
[21] C.-S. Chen, Y. Fujimoto, G. Girdaukas, C.J. Sih, J. Am. Chem. Soc. 104 (1982) 7294–7299.
[22] J.L.L. Rakels, A.J.J. Straathof, J.J. Heijnen, Enzyme Microb. Technol. 15 (1993) 1051–1056.
[23] R.S. Phillips, Enzyme Microb. Technol. 14 (1992) 417–419.
[24] R.S. Phillips, Trends Biotechnol. 14 (1996) 13–16.
[25] H.M. Berman, J. Westbrook, Z. Feng, G. Gilliland, T.N. Bhat, H. Weissig, I.N. Shindyalov, P.E. Bourne, Nucleic Acids Res. 28 (2000) 235–242.
[26] J. Uppenberg, M.T. Hansen, S. Patkart, T.A. Jones, Structure 2 (1994) 293–308.
[27] A.D. MacKerell Jr., D. Bashford, M. Bellott, R.L. Dunbrack Jr., J.D. Evanseck, M.J. Field, S. Fischer, J. Gao, H. Guo, S. Ha, D. Joseph-McCarthy, L. Kuchnir, K. Kuczera, F.T.K. Lau, C. Mattos, S. Michnick, T. Ngo, D.T. Nguyen, B. Prodhom, W.E. Reiher III, B. Roux, M. Schlenkrich, J.C. Smith, R. Stote, J. Straub, M. Watanabe, J. Wiorkiewicz-Kuczera, D. Yin, M. Karplus, J. Phys. Chem. B 102 (1998) 3586–3616.
[28] S.C. Lovell, J.M. Word, J.S. Richardson, D.C. Richardson, Proteins 40 (2000) 389–408.
[29] M.L. Connolly, Science 221 (1983) 709–713.
[30] H.J.C. Berendsen, J.P.M. Postma, W.F. Van Gunsteren, A. Dinola, J.R. Haak, J. Chem. Phys. 81 (1984) 3684–3690.
[31] J. Ottosson, L. Fransson, K. Hult, Protein Sci. 11 (2002) 1462–1471.
[32] A.O. Magnusson, M. Takwa, A. Hamberg, K. Hult, Angew. Chem. Int. Ed. 44 (2005) 4582–4585.
[33] J. Pleiss, M. Fischer, R.F. Schmid, Chem. Phys. Lipids 93 (1998) 67–80.